

Southern Ocean Pleistocene calcareous nannofossil events: calibration with isotope and geomagnetic stratigraphies

J.-A. Flores^{a,*}, R. Gersonde^b, F.J. Sierro^a, H.-S. Niebler^c

^aUniversidad de Salamanca, Departamento de Geología, 37008 Salamanca, Spain

^bAlfred Wegener Institute for Polar and Marine Research, D-27568 Bremerhaven, Germany

^cBremen University, Department of Geoscience, Klagenfurter Strasse, D-28359 Bremen, Germany

Received 3 February 2000; accepted 26 June 2000

Abstract

Several cores recovered from the northern belt of the Southern Ocean were analysed to study the Pleistocene calcareous nannofossil records. Calcareous nannofossil events previously described in medium and low latitudes were identified and calibrated with the oxygen isotope and geomagnetic time scales. Although sedimentation rates, hiatuses and degree of calcareous nannofossil preservation sometimes prevent the identification and/or accurate calibration of some of these events, a useful stratigraphic framework was obtained. The possibility of using these calibrated events from high to low latitudes facilitates correlations and should facilitate isotope event identification in a region with low temperature, where calcareous plankton stratigraphies are in general restricted. In general, Pleistocene southern high latitude calcareous nannofossil events show synchronism with those observed in warm and temperate surficial waters. Small discrepancies in the assigned ages are sometimes related to low sampling resolution due to low sedimentation rates. The first occurrence (FO) of *Emiliania huxleyi* and the last occurrence (LO) of *Pseudoemiliania lacunosa* are observed in Marine Isotope Stages (MIS) 8 and 12, respectively. A reversal in abundance between *Gephyrocapsa muelleriae* and *E. huxleyi* is observed close to the MIS 4/5 boundary. MIS 6 is characterised by an increase in *G. muelleriae* and MIS 7 features a dramatic decrease in the proportion of *Gephyrocapsa caribbeanica*. This latter species began to increase its proportions from the MIS 13/14 boundary to MIS 13, showing diachronism between the different sites. The LO of *Reticulofenestra asanoi* is observed at MIS 22, confirming this event as a global synchronous reference datum. By contrast, the FO of *R. asanoi* occurs at MIS 35 and is diachronous with the existing data from other oceanic regions. A re-entry of medium sized *Gephyrocapsa* (3–5 μm maximum diameters) can be identified in some cores close to MIS 25; although the low abundance of this taxon prevents an accurate calibration, it may be concluded that this event is diachronous as compared with the existing low-latitude data. The LO of large morphotypes of *Gephyrocapsa* is well correlated with MIS 37, showing synchronism with other oceanic regions, whereas the FO of this species is not well calibrated due to the absence of age-control points. © 2000 Elsevier Science B.V. All rights reserved.

Keywords: Southern Ocean; Pleistocene; calcareous nannofossils; biostratigraphy; isotope stratigraphy; geomagnetic stratigraphy

1. Introduction

Over the last decades calcareous nannofossils have shown excellent potential in Pleistocene biostratigraphy. Improved isotope and magnetostratigraphic data have permitted the calibration of the calcareous

* Corresponding author. Tel.: +34-923-294497; fax: +34-923-294514.

E-mail address: flores@gugu.usal.es (J.-A. Flores).

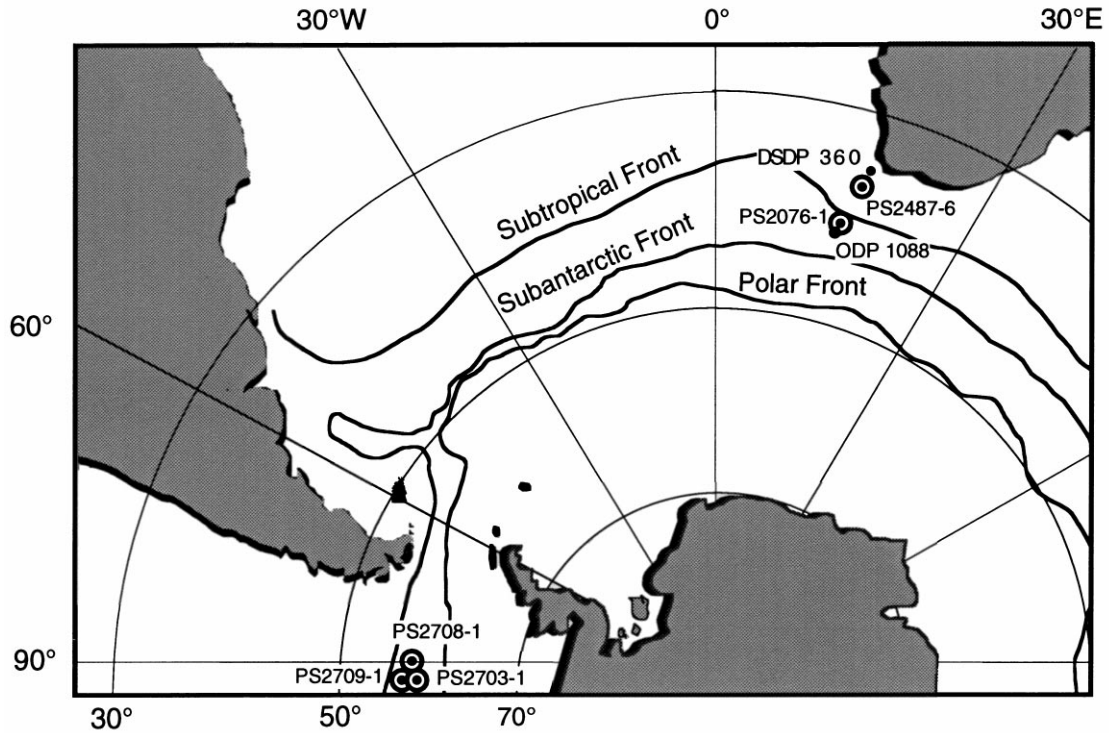


Fig. 1. Location of cores used in this study and main oceanographic features.

nannofossil data, allowing a more precise correlation between different regions, and consequently, the dating of paleoceanographic events. Accurate age determination and the evaluation of synchrony of micropaleontological data are essential in paleoceanographic analyses to provide age-control points, which then help to infer ages or to interpret isotope stratigraphy. Such analyses are also important in paleoecological studies on the Pleistocene, a time interval of special relevance in the understanding of climate evolution and cyclicity. Examples of these biochronological data come from Thierstein et al. (1977), Gartner (1977), Pujos-Lamy (1977), Matsuoka and Okada (1990), Giraudeau and Pujos (1990), Wei (1993), Raffi et al. (1993), Weaver and Thomson (1993), Pujos and Giraudeau (1993), Wells and Okada (1997), Hine and Weaver (1998) and Bollmann et al. (1998) among others. However, most of the above studies focus on middle- and low-latitude sections and only few of them are based on material recovered in the Southern Ocean, which plays an important role

in climatic and oceanic evolution (Kennet and Barron, 1992; Shipboard scientific Party Leg 177, 1999). The present study focuses on the identification and calibration of calcareous nannofossil biostratigraphic data in order to improve the stratigraphic framework for southern high-latitude paleoceanographic studies.

The zonations of Martini (1971) and Okada and Bukry (1980) for Quaternary nannofossil Pleistocene biostratigraphy were improved when quantitative data and new deep-sea material became available. Several authors, cited previously in this section, generated new higher-resolution schemes, in most cases calibrated chronologically. Worldwide events were observed, mainly in tropical and in temperate water masses, due to the cosmopolitan characteristics of most of the species involved (Raffi et al., 1993; Wei, 1993).

As mentioned above, stratigraphic studies carried out on Pleistocene material from the Southern Ocean in general disclose low sedimentation rates and/or hiatuses of different stratigraphic extent (Wise and

Table 1
Core locations and name of expedition leg

Core designation	Location	Water depth (m)	<i>Polarstern</i> expedition
<i>Atlantic sector</i>			
PS2487-6	35°49.2' S/18° 05.4'E	2950	ANTARKTIS-XI/2 1993–1994 Gersonde et al. (1995)
PS2076-1	41°08.12' S/13°28.87' E	2086	ANTARKTIS-IX/4 1991 Bathmann et al., 1992
<i>Pacific sector</i>			
PS2708-1	57° 46.8' S/90° 59.9' W	3965	ANTARKTIS-XII/4 1995 Gersonde, in press
PS2709-1	57° 35.4'/S 91° 13.2' W	2707	ANTARKTIS-XII/4 1995 Gersonde, in press
PS2703-1	57°66.1' S/91° 10.8' W	2747	ANTARKTIS-XII/4 1995 Gersonde, in press

Wind, 1977; Wise, 1983; Crux, 1991; Wei and Wise, 1992). In other cases, at these latitudes the calcareous plankton is in general diluted by siliceous organisms or is affected by dissolution. Consequently, the number of sections available is restricted. To these factors should be added restrictions in ecological calcareous nannofossil marker species. Alternative quantitative events to the “standard” can improve stratigraphic resolution in this region.

2. Material and methods

2.1. Core location and lithology

The five piston cores studied were recovered during the RV *Polarstern* cruises ANT IX/4, XI/2 and XII/4 in the Atlantic and the Pacific sectors of the Southern Ocean (Bathmann et al. 1992; Gersonde et al., 1995) (Fig. 1, Table 1).

Core PS2487-6 was recovered on the continental slope south of the African Cape and thus represents the only core addressed in this paper that originates from southern subtropical waters. The core location is in the vicinity of DSDP Site 360 (Bolli et al., 1978) and consist of foraminiferal ooze alternating with mud and nannofossil oozes. The isotope and nannofossil stratigraphy obtained from the upper 9 m of PS2487-6, which cover the past ca. 1 My, was described in detail by Flores et al. (1999), including a study of the Pleistocene paleoceanographic evolution of the Agulhas retroflexion. Here we add data from the lowermost 3 m of the core. Core PS2076-1 originates from the crest of the northern Agulhas Fracture Zone Ridge, in the

northern Subantarctic Zone of the Antarctic Circumpolar Current (ACC). The core location is close to ODP Site 1088, drilled during Leg 177 (Shipboard Scientific Party Leg 177, 1999). The isotope and planktonic foraminifera stratigraphy of PS2076-1 from Marine Isotope Stage (MIS) 1 to 20 is reported in Niebler (1995). Here, we interpret this stratigraphy in the section below MIS 20.

Cores PS2703-1, PS2708-1 and PS2709-1 were collected from the San Martin Seamounts in the Bellingshausen Sea. This area, located in the Polar Front Zone of the ACC, has been reported to have been affected by the late Pliocene impact of the “Eltanin” asteroid (Gersonde et al., 1997). The Pleistocene sediments of Cores PS2709-1 and PS2703-1 are calcareous ooze consisting of well-preserved calcareous nannofossil and foraminiferal assemblages, which allows the establishment of stable isotope records in the former (Table 2). Core PS2708-1, recovered at greater water depths from the seamount flank, shows evident carbonate dissolution that prevents the establishment of a well-established isotope record. However, the calcareous nannofossil preservation is moderate throughout most of the Pleistocene section of PS2708-1. The geomagnetic data for PS2708-1 and PS2709-1 are from Gersonde et al. (1997).

For the isotopic record we used the age model of Tiedemann et al. (1994) for the last MIS 48. For geomagnetic calibration we followed the proposal of Cande and Kent (1992). Boundaries between well-identified isotope events, paleomagnetic reversals, and sometimes worldwide synchronous biostratigraphic data were used to estimate sedimentation rates.

Table 2
 $\delta^{18}\text{O}$ values of *Neogloboquadrina pachyderma* (sinistral) in core PS2709-1

Depth (cm)	$\delta^{18}\text{O}$ PDB <i>Neogloboquadrina pachyderma</i>	Depth (cm)	$\delta^{18}\text{O}$ PDB <i>Neogloboquadrina pachyderma</i>	Depth (cm)	$\delta^{18}\text{O}$ PDB <i>Neogloboquadrina pachyderma</i>
6	3.79	576	3.36	1136	2.99
16	4.06	586	3.51	1146	2.80
26	4.01	595	3.28	1156	3.24
36	3.86	606	3.24	1166	3.53
39	3.42	616	3.63	1176	3.56
46	3.95	626	3.13	1186	3.18
56	3.7	636	2.75	1196	3.62
66	3.69	646	2.69	1206	3.31
76	2.88	656	2.89	1216	3.14
86	3.42	666	3.17	1226	2.69
96	3.53	676	3.35	1236	2.29
106	3.57	686	2.84	1246	2.97
116	3.99	696	2.88	1256	3.70
136	3.98	706	2.9	1276	3.84
146	3.74	716	2.76	1286	3.40
156	3.68	726	2.64	1296	3.37
166	3.83	736	2.99	1306	2.88
176	3.88	746	3.52	1316	3.29
186	3.88	756	3.34	1326	3.03
196	3.58	766	2.92	1336	2.81
206	3.71	786	2.87	1346	3.10
216	2.80	796	3.11	1356	2.99
226	2.86	806	3.16	1366	3.34
236	2.77	816	3.04	1376	3.24
255	2.88	826	3.00	1386	3.03
296	2.72	836	3.04	1396	2.99
316	3.09	846	2.89	1406	2.75
326	3.44	856	3.29	1416	3.15
336	3.65	866	2.93	1426	3.47
346	3.11	876	3.03	1436	3.10
356	2.89	906	3.55	1446	2.92
366	3.16	916	3.41	1456	2.87
376	3.28	936	2.46	1466	3.10
386	3.21	946	3.04	1476	2.68
396	3.16	956	3.24	1486	3.13
406	3.27	966	3.27	1496	2.69
416	3.32	976	3.46	1506	3.24
426	3.17	986	2.84	1516	3.28
436	3.20	996	3.17	1526	3.09
446	2.97	1006	3.63	1536	3.12
456	2.90	1016	3.07	1546	3.00
466	3.84	1026	3.25	1566	3.17
476	4.15	1036	3.09	1576	3.13
486	4.00	1056	2.94	1586	3.19
496	3.73	1065	3.52	1596	3.11
516	3.85	1076	3.73	1606	3.33
526	3.53	1086	3.65	1616	3.04
536	3.34	1096	3.36	1618	3.12
546	2.85	1106	3.05	1626	3.07
556	3.02	1116	3.45	1636	2.92
566	2.91	1126	3.45	1646	2.85

2.2. Calcareous nanofossil preparation technique and estimation of abundances

Smear slides were made directly from unprocessed samples and examined with a light microscope at 1250x. The abundance of calcareous nanofossils was estimated following the criteria reported by Raffi and Flores (1995), summarised as follows: A = >50 nannoliths per field of view, C = 1–50 nannoliths per field of view. Samples with less than one specimen per field of view were not included in the Appendix Tables A1–A5. The ranking of preservation was established as: G = good, M = moderate, and P = poor. The relative abundance of taxa or morphotypes were: V = very abundant (>50%); A = abundant (>20 <50%); C = common (>10 <20%); F = few (>1 <10%); R = rare (<1%).

The slides are stored in the archives of the Micropaleontological Collections of the University of Salamanca and the Alfred Wegener Institute.

2.3. Stable isotope analyses techniques

For the establishment of a stable isotope record in Core PS2709-1 five specimens of *Neogloboquadrina pachyderma* (sinistral forms) ranging in size between 250 and 300 μm , were picked from each sample at a sample spacing of 10 cm. Isotope measurements were performed at the Alfred Wegener Institute with a Finnigan Modern Analogue Technique 251 mass spectrometer coupled to an automatic preparation device operated under the supervision of Dr A. Mackensen. Standard deviations of measurements were <0.09‰ for oxygen. Data were related to the PDB standard through repeated analyses of National Bureau of Standards isotopic reference material 19 (Hut, 1987).

3. Calcareous nanofossil taxonomy

The species involved in this study are mainly included within the family Noelaerhabdaceae (Reticulofenestrids including the genera *Emiliania*, *Pseudoemiliania*, *Gephyrocapsa* and *Reticulofenestra*) (Thierstein et al., 1977; Pujos-Lamy, 1977; Wei, 1993; Raffi et al., 1993; Weaver and Thomson, 1993). However, the taxonomy of this group is complex and confusing, mainly due to a proliferation

of species names and morphotypes. Here we adopted the ideas of Raffi et al. (1993) for the morphological features of Gephyrocapsids. We introduce other morphotype or species markers following similar rules concerning diameter, bridge angle, etc, which are readily identifiable under the polarised microscope. The morphological features and terminology used here are summarised in Table 3. A complete list of the taxa studied is included in the Taxonomic Appendix.

4. Results and analyses

For the present study, a detailed calcareous nanofossil range chart for Core PS2487-6 was constructed (see Appendix Table A1). Quantitative analyses for the upper 500 cm (last 13 MIS) have been presented previously by Flores et al. (1999). Here we include analyses from the base of the core. Calcareous nanofossils from core PS2487-6 are abundant, and their preservation is good. Fig. 2 and Table 4 show the calcareous nanofossil events and their relationship with the isotope curve. A hiatus identified close to 500 cm discloses two intervals. The uppermost part shows a continuous sequence of events in which isotope stages are well defined. However, the lower part is not well defined isotopically, and consequently the calibration of calcareous nanofossil events is tentative.

The calcareous nanofossil abundance of core PS2076-1 is variable, ranging from high to low, and the degree of preservation is moderate to good. The range chart data can be found in the Appendix Table A2. Fig. 3 shows the correspondence between the calcareous nanofossil events and isotope stages. A continuous sequence can be observed from MIS 25 to the Holocene. Unfortunately, below the 675 cm sample the isotope signal is difficult to interpret, especially when compared with the nanofossil data.

Appendix Tables A3 and A4 show the results from cores PS2709-1 and PS2703-1. A similar calcareous nanofossil record is observed in both cores, although some intervals from the former core are more affected by dissolution. Fig. 4 shows a relatively good isotopic and geomagnetic record for these cores, allowing identification of the last 37 isotope stages and their correlation with nanofossil events. Only below the

Table 3
Terminology adopted and equivalences for calcareous nannofossil taxa and morphotypes

This study:	<i>G. oceanica</i>	<i>G. muelleriae</i>	<i>G. caribbeanica</i>	Small <i>Gephyrocapsa</i>	Medium <i>Gephyrocapsa</i> + <i>G. omega</i>	Large <i>Gephyrocapsa</i>	<i>R. asanoi</i>
Bridge angle:	> 50°	< 25°	Closed central area	–	~90°	–	–
Maximum diameter:	> 3 µm	> 3 µm	> 3 µm	< 3 µm	>3<5.5 µm open central area	>5.5 µm closed central area	>6 µm
Author equivalence							
Bukry, 1973	–	–	–	–	<i>G. omega</i>	–	–
Thierstein et al., 1977	–	<i>G. caribbeanica</i>	–	–	–	–	–
Bréhéret, 1978	<i>G. oceanica</i>	<i>G. muelleriae</i>	<i>G. caribbeanica</i>	<i>G. aperta</i> , <i>G. ericsonii</i>	–	–	–
Takayama & Sato, 1987	–	–	–	–	–	–	<i>Reticulofenestra</i> sp. A
Santleben, 1980	<i>G. oceanica</i>	<i>G. muelleriae</i>	<i>G. caribbeanica</i>	Several species	–	–	–
Matsuoka & Okada, 1990	<i>G. sp. D</i> (large)	<i>G. sp. D</i>	<i>Gephyrocapsa</i> sp. D (small)	<i>Gephyrocapsa</i> spp. (small)	<i>Gephyrocapsa</i> sp. C	<i>Gephyrocapsa</i> sp. B	<i>Reticulofenestra</i> sp. A
Sato & Takayama, 1992	–	–	–	–	<i>G. parallela</i>	Large <i>Gephyrocapsa</i>	<i>R. asanoi</i>
Raffi et al., 1993	Medium <i>Gephyrocapsa</i>	Small <i>Gephyrocapsa</i>	Small <i>Gephyrocapsa</i>	Small <i>Gephyrocapsa</i>	<i>G. omega</i>	Large <i>Gephyrocapsa</i>	–
Jordan et al., 1996	<i>G. oceanica</i>	<i>G. muelleriae</i>	–	<i>G. aperta</i> , <i>G. ericsoni</i>	–	–	–
Bollmann, 1997	<i>Gephyrocapsa</i> large + equatorial	<i>Gephyrocapsa</i> cold	<i>Gephyrocapsa</i> oligotrophic	<i>Gephyrocapsa</i> minute	–	–	–

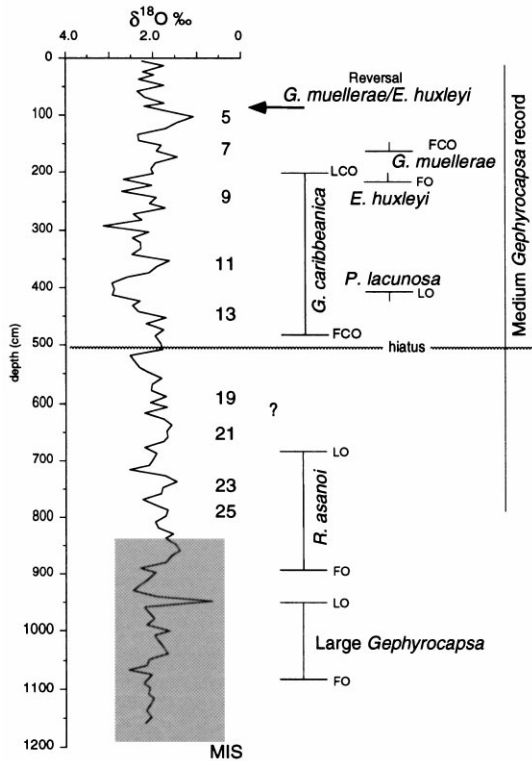


Fig. 2. Calcareous nannofossil events identified in core PS2487-6. The $\delta^{18}\text{O}$ curve is from Flores et al. (1999). The shaded area represents an interval with low isotope resolution. LO: last occurrence; FO: first occurrence; LCO: last common occurrence; FCO: first common occurrence. MIS: marine isotope stages.

1200 cm sample does the isotope resolution preclude accurate identification of the isotope stages.

The calcareous nannofossil assemblages observed in Core PS2708-1 are less abundant than the above-mentioned cores. Together with a poor preservation, this hinders the identification of certain calcareous nannofossil events. However, those nannofossil events that could be identified are well calibrated owing to the core's good geomagnetic pattern (Fig. 5).

A list of the calcareous nannofossil events used in this study, their location (depth), and a correlation with isotope and/or geomagnetic events in each are shown in Table 4, and plotted in Figs. 6 and 7. The small discrepancies observed in some of the events identified could be due to sampling resolution and/or the precision of the age model adopted for each site.

5. Discussion

5.1. *Emiliana huxleyi* Acme base

The base of the *Emiliana huxleyi* Acme is a diachronous event and is difficult to recognise in certain areas of the ocean (Jordan et al., 1996). Gartner (1977) dated the *E. huxleyi* Acme bottom at 70 ky. Thierstein et al. (1977) proposed the use of the so-called "Reversal in abundance of *Gephyrocapsa caribbeanica* – *E. huxleyi*" (= *Gephyrocapsa muellerae* – *E. huxleyi*, dated at 73–85 ky), as a biostratigraphic event. This event was identified by Gard and Crux (1991) as having occurred during the MIS 4/5 boundary in ODP Site 704, in the Subantarctic from the Atlantic sector. In several areas this event coincides with a regular increase in *E. huxleyi* and is considered to be the bottom of the *E. huxleyi* Acme zone (or Zone of Dominance). Other authors have traced this event to the time where *E. huxleyi* became the dominant species. For example, in the Arctic Ocean this occurred between 61 to 40 ky ago (Gard, 1989; Novaczyk and Baumann, 1992). The meaning of "Acme" or "Zone of Dominance" is confusing because in different regions the proportion of *E. huxleyi* may be altered with respect to other species (ecologically controlled), or due to a relative reduction arising from dissolution (Thierstein et al., 1977).

A reversal in the abundance of *Gephyrocapsa muellerae/Emiliana huxleyi* can be observed in Cores PS2487-1 and PS2076-1 at the MIS 4/5 boundary (Figs. 2 and 3; Appendix Tables A1 and A2). In Core PS2709-1, this reversal is identified at MIS 5, corresponding to low $\delta^{18}\text{O}$ values. The same event is observed in core PS2703-1 at the same relative position as in the other cores (Fig. 4; Appendix Table A3). Close to this event, different authors have identified other events. Thus, Jordan et al. (1996) observed a prominent abundance peak in *Gephyrocapsa oceanica* at MIS 5e in the Tropical Atlantic. Gard and Crux (1991) identified a weak peak in *Gephyrocapsa* spp. during the whole of MIS 5, together with a peak of *Calcidiscus leptoporus* at ODP Site 704 (Meteor Rise). In Core PS2487-6, an proportional increase in *G. oceanica* and *C. leptoporus* can be seen observed at around 125 cm (Flores et al., 1999), although it is not clear in the other cores studied.

Table 4
Calcareous nannofossil events in the cores studied and their calibration to marine isotope stages and magnetostratigraphy

Nannofossil event	PS2487-6		PS2076-1		PS2708-1		PS2709-1			PS2703-1
	MIS	cm	MIS	cm	Chron	cm	MIS	Chron	cm	cm
Reversal <i>G. muellerae</i> / <i>E. huxleyi</i>	4/5	90–100	4/5	67–77	–	–	–	–	–	78–88
FCO <i>G. muellerae</i>	6/7	150–160	6/7	137–147	Cln	Dissolved	6/7	Cln	140–145	128–138
LCO <i>Gephyrocapsa caribbeanica</i>	7	200–210	7	157–167	Cln	Dissolved	7	Cln	145–150	128–138
FO <i>Emiliana huxleyi</i>	8	210–220	8	187–197	Cln	111–132	8	Cln	150–155	138–148
LO <i>Pseudoemiliana lacunosa</i>	12	400–410	12	297–307	Cln	170–203	12	Cln	380–390	428–438
FCO <i>Gephyrocapsa caribbeanica</i>	13	465–470	14/15	357–367	Cln	–	14/13	Cln	416–422	448–458
LO <i>Reticulofenestre asanoi</i>	22	685–695	22	577–587	Clr.1r	347–363	22	Clr.1r	725–730	818–828
Re-entry medium <i>Gephyrocapsa</i>	25	765–785	25	647–657		363–370	25		770–780	908–918
FO <i>R. asanoi</i>	35?	895–905	35?	757–767	Cl1.2r.1r bottom	600–630	35	Clr.2r.1r bottom	1060–1065	1123–1173
LO Large <i>Gephyrocapsa</i>	37?	945–955	37?	777–787	Cl1.2r.2r top	690–711	37?	Clr.2r.2r top	1090–1095	1233–1240
FO Large <i>Gephyrocapsa</i>	?	1073–1085	?	907–917	Clr.2r.2r	810–820	?	Clr.2r.2r	1270–1275	1510–1520

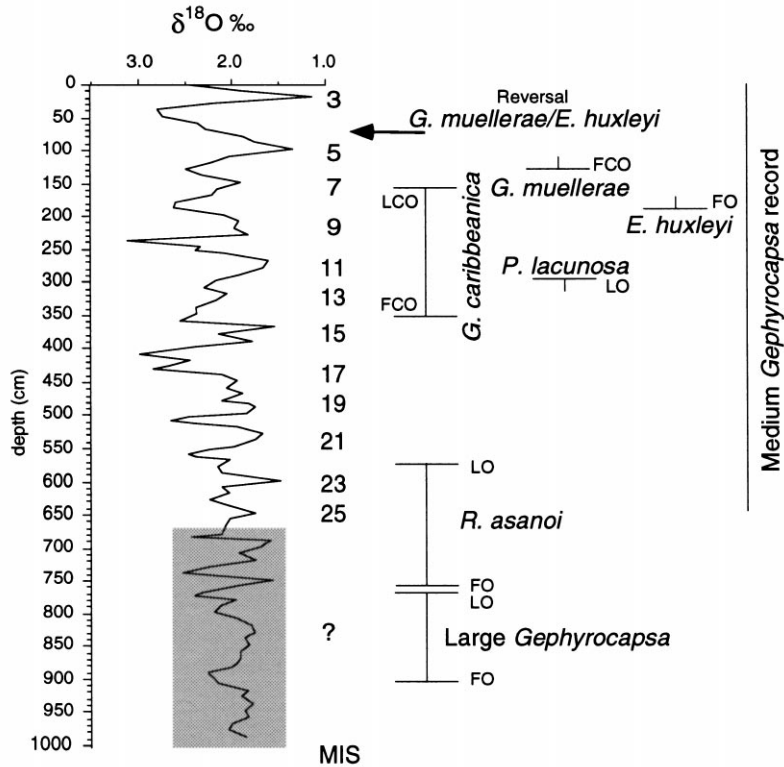


Fig. 3. Calcareous nannofossil events identified in core PS2076-1. $\delta^{18}\text{O}$ is from Niebler (1995). The shaded area represents an interval with low isotope resolution. LO: last occurrence; FO: first occurrence; LCO: last common occurrence; FCO: first common occurrence. MIS: marine isotope stages.

5.2. First occurrence of *Emiliana huxleyi*

The first occurrence (FO) of *Emiliana huxleyi* was dated by Thierstein et al. (1977) at 268 ky (late in MIS 8). The relatively easily dissolved placoliths of *E. huxleyi* may hinder the identification of this FO, especially when working with the light microscope. However, this FO can be positively identified in Cores PS2076-1, PS2487-6, PS2709-1 and PS2703-1. Poor nannofossil preservation and the lack of an isotope curve preclude a good calibration of this event in Core PS2708-1 (Figs. 2–5; Table 4; Appendix Tables A1–A5).

5.3. First common occurrence of *Gephyrocapsa muellerae* and last common occurrence of *Gephyrocapsa caribbeanica*

The first common occurrence (FCO; continuous

record after a significant increase in abundance) of *Gephyrocapsa muellerae* occurs in the MIS 6 (at ca. 170 ky) and the last common occurrence (LCO; dramatic reduction) of *Gephyrocapsa caribbeanica* at the bottom of MIS 7 (Weaver, 1983; Weaver and Thomson, 1993; Pujos and Giraudeau, 1993; Bollmann et al., 1998; Flores et al., 1999); for systematic criteria see Table 2. The LCO of *G. caribbeanica* is equivalent to the increase in the so-called small *Gephyrocapsa* sp. D observed by Matsuoka and Okada (1990). In our material, the FCO of *G. muellerae* is identified at the MIS 6/7 boundary in Cores PS2487-6 and PS2076-1 (Figs. 2 and 3; Appendix Tables A1 and A2) and at the base of MIS 6 in Core PS2709-1 (Fig. 4; Appendix Table A3). Pujos and Giraudeau (1993) defined this event as an increase of “open *Gephyrocapsa*” from the top of MIS 7 or base of MIS 6 in the North Atlantic and Southern Ocean; this allows us to infer a global synchronism.

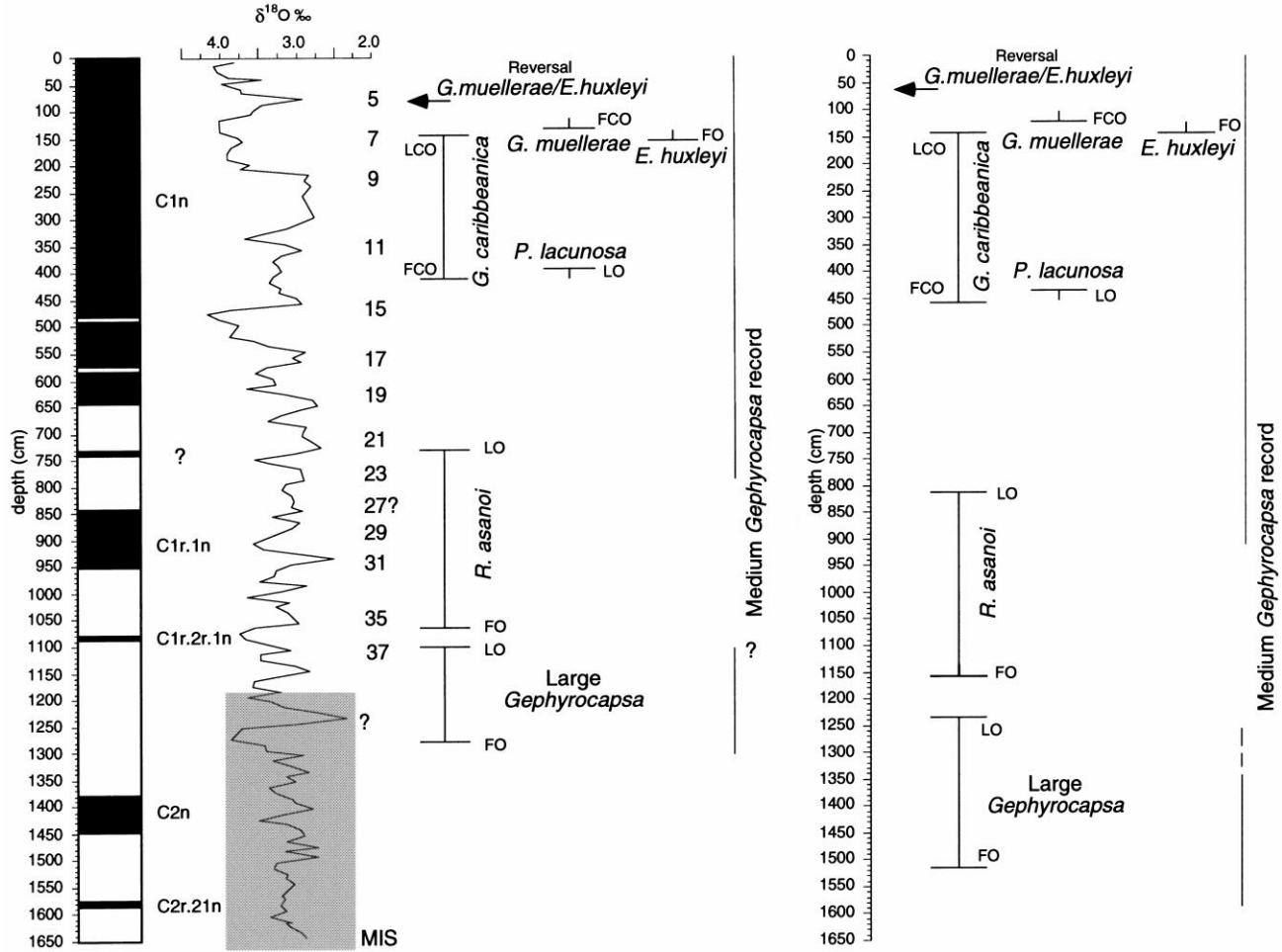


Fig. 4. Calcareous nannofossil events identified in cores PS2709-1 and PS2703. Paleomagnetic data are from Gersonde et al. (1997). $\delta^{18}\text{O}$ data are shown in Table 2. LO: last occurrence; FO: first occurrence; LCO: last common occurrence; FCO: first common occurrence. MIS: marine isotope stages.

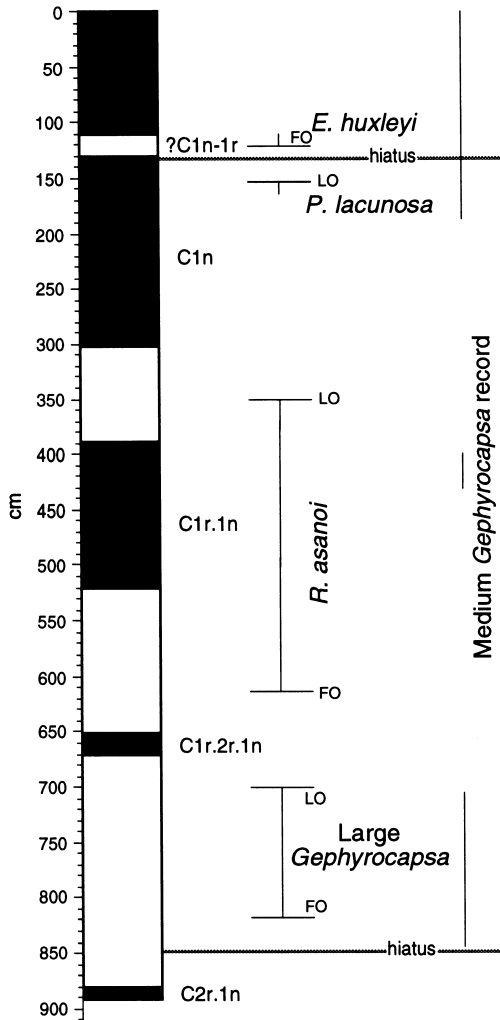


Fig. 5. Calcareous nannofossil events identified in core PS2708-1. Paleomagnetic data are from Gersonde et al. (1997). LO: last occurrence; FO: first occurrence; LCO: last common occurrence; FCO: first common occurrence. MIS: marine isotope stages.

The LCO of *Gephyrocapsa caribbeanica* is close to the well-dated FO of *Emiliania huxleyi* at MIS 8. Here, a clear reduction in the abundance of *G. caribbeanica* occurs at the base of MIS 7 in Cores PS2487-6, PS2076-1, PS2709-1 and PS2703-1, showing good synchrony (Figs. 2–4; Table 4; Appendix Tables A1–A4). Pujos and Giraudeau (1993) reported a dramatic reduction in “closed *Gephyrocapsa*” (which we consider equivalent to *G. caribbeanica*) during MIS 8, but progressively

decreasing at the base of MIS 7, in North Atlantic, Pacific Ocean and Southern Ocean. Consequently, the existing data agree with the notion of a global synchronism.

5.4. Last occurrence of *Pseudoemiliania lacunosa*

Thierstein et al. (1977) identified the globally synchronous last occurrence (LO) of *Pseudoemiliania lacunosa* at the middle of MIS 12. Gard and Crux (1991) observed very low proportions of this species in high latitudes in ODP Site 704. This event has also been reported to occur at the same time in relatively high latitudes by Wei (1993), in agreement with own observations (Figs. 2–7, Table 4; Appendix Tables A1–A5). A clear increase in the abundance of *Gephyrocapsa caribbeanica* can be identified during MIS 13 in Core PS2487-6, and MIS 13/14 boundary at cores PS2709-1 and PS2076-1 (Figs. 2–4; Table 4; Appendix Tables A1–A3). Several authors have reported events that may be equivalent to this, and although the nomenclature may be confusing, it seems convenient to explain the status in some detail (see also systematic equivalencies in Table 3). At this level, Matsuoka and Okada (1990) observed a progressive increase in *Gephyrocapsa* sp. D as well as a reduction in *Gephyrocapsa* sp. C. An increase in “closed *Gephyrocapsa*” (equivalent event) has been reported by Pujos and Giraudeau (1993) in the North Atlantic during MIS 13. At ODP Site 704 Gard and Crux (1991) observed an interval of dominance of small placoliths (<5 μm) between MIS 9 and 13, with a reduction in glacial stages (MIS 10 and 12). This event corresponds to the base of the *Gephyrocapsa* dominance interval described by Bollmann et al. (1998), and the interval of dominance of *G. caribbeanica* reported by Flores et al. (1999). According to the available data, the FCO of *G. caribbeanica* is therefore a synchronous event, although in the cores studied here the isotope analyses are not very accurate (Figs. 2–4).

5.5. Last occurrence of *Reticulofenestra asanoi*

The LO of *Reticulofenestra asanoi* is well-established (Sato and Takayama, 1992) and is a synchronous event in low and relatively high latitudes, that occurred late in MIS 22 (Wei, 1993). This is also apparent in relatively high latitude material. In our

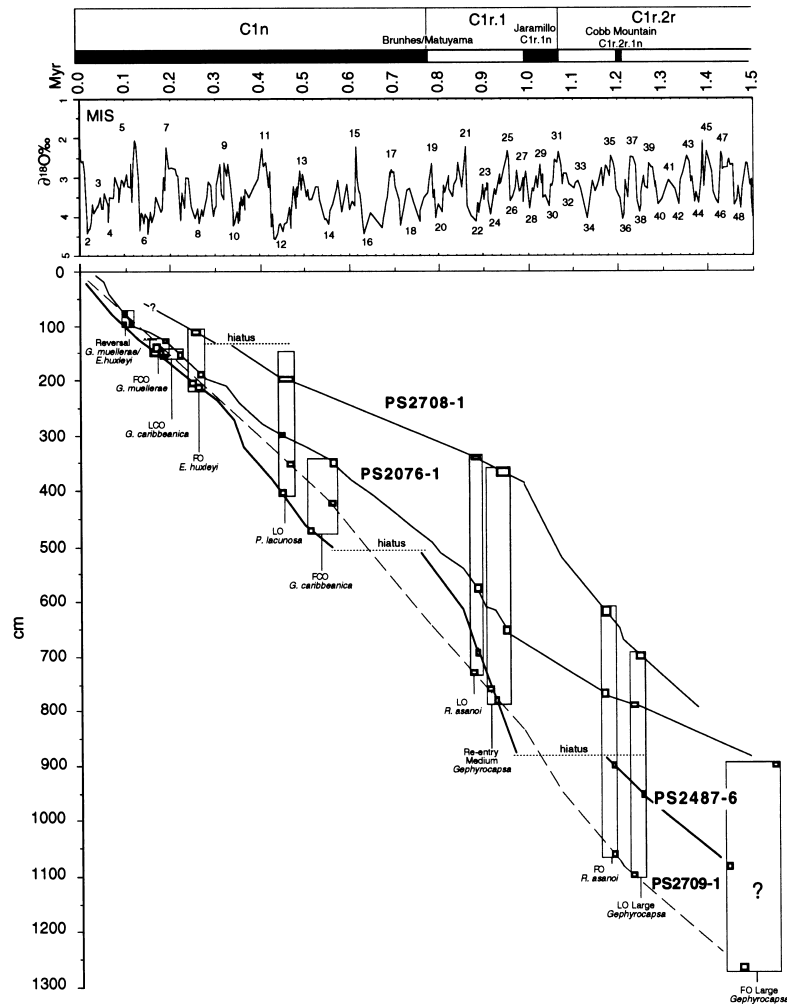


Fig. 6. Schema showing estimated sedimentation rates. Calcareous nannofossil event calibrations were performed with paleomagnetic data (after Cande and Kent, 1992) and $\delta^{18}\text{O}$ curve (Tiedemann et al., 1994). MIS: marine isotope stages.

cores, this event also correlates with MIS 22 in Core PS2709-1. Taking into account the paleomagnetic record, the LO of *R. asanoi* is centered at subchron C1r.1r in Cores PS2709-1 and PS2708-1 (Figs. 4–7; Table 4; Appendix Tables A3 and A5). Peaks of *R. asanoi* recorded after the LO of *Pseudoemiliana lacunosa* are interpreted as being reworked.

5.6. Re-entry of medium *Gephyrocapsa*

Raffi et al. (1993) reported the re-entry of the

so-called Medium *Gephyrocapsa* (mainly *Gephyrocapsa omega* = *Gephyrocapsa parallela* = *Gephyrocapsa* sp. C; see Table 3) between MIS 29 and 16, with a marked degree of diachronism. The FO of *Gephyrocapsa* sp. C (Matsuoka and Okada, 1990) was recorded by Wei (1993) in high latitudes in the North Atlantic between MIS 25 and 26, and close to MIS 15 and 16 in high latitudes in the South Pacific, showing a similar degree of diachronism as that reported by Raffi et al. (1993). In our cores the re-entry of medium *Gephyrocapsa* is not easy to recognise

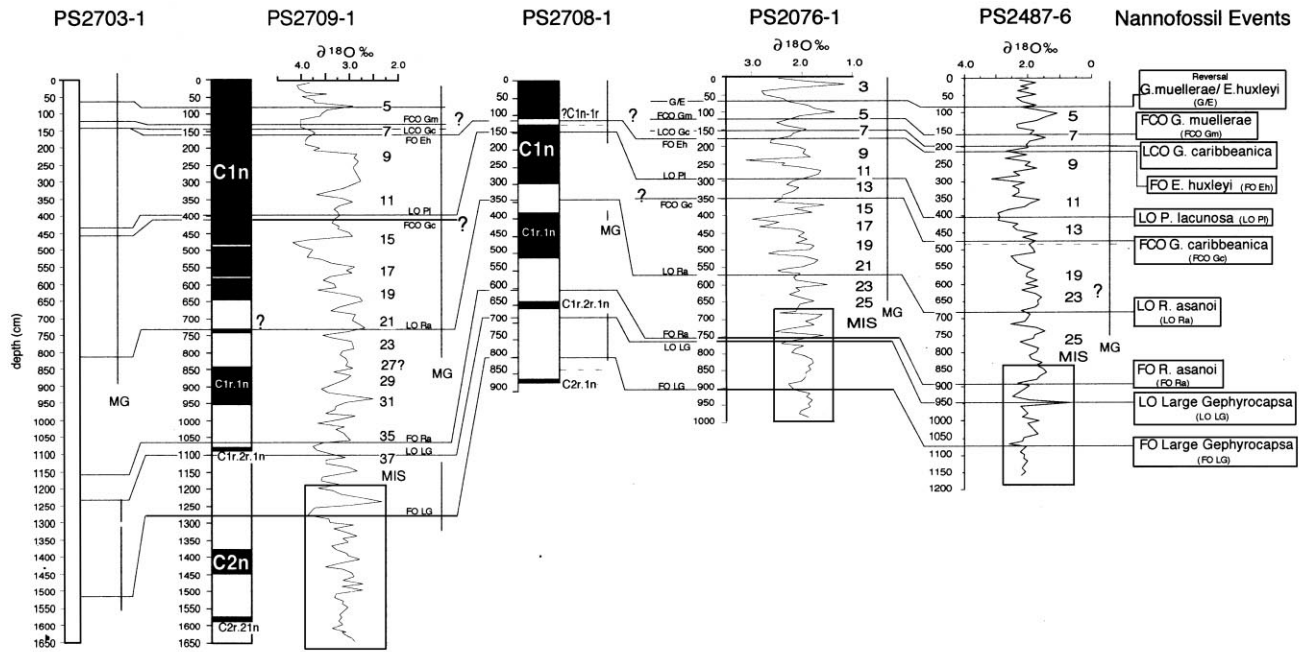


Fig. 7. Calcareous nannofossil events and their correlation with the isotopic and geomagnetic stratigraphies in the studied cores. LO = last occurrence; FO = first occurrence; LCO = last common occurrence; FCO = first common occurrence. MG = medium *Gephyrocapsa* (the vertical line represent the record of this group along the core). MIS — marine isotope stage. The dashed line represents hiatus. The boxed area in the isotopic curves represents intervals with low isotope resolution.

owing to the low proportions at which the morphotype is recorded. A re-entry of medium sized *Gephyrocapsa* is observed close to MIS 25 in cores PS2487-6, PS2076-1 and PS2709-1 (Figs. 3 and 4; Appendix Tables A1 and A3). In Core PS2487-6, a typical *G. parallela* morphotype can be observed, with a marked peak close to MIS 25 (Flores et al. 1999) (Fig. 2; Appendix Table A1). In core PS 2708-1 this morphotype is very scarce and the identification of its re-entry is not easy. However, as shown in Fig. 5 (Appendix Table A5), a pulse of this species can be observed during subchron C1r.1n, close to the assigned age for MIS 25. According to our data, the re-entry of Medium *Gephyrocapsa* was a synchronous event in the Southern Ocean (Figs. 6 and 7), although dissolution prevents good definition in high latitudes.

5.7. First occurrence of *Reticulofenestra asanoi*

The FO of *Reticulofenestra asanoi* is not easy to identify owing to the occurrence of intermediate forms between this species and small *Reticulofenestrids* (Wei, 1993). We therefore only consider specimens with maximum diameters larger than 6 μm (Table 3), following the original description of Sato and Takayama (1992). Taking into account this problem, Wei (1993) observed the FO of the species between MIS 35 and 29. Sato and Takayama (1992) dated the event at 1.06 Ma (around MIS 30) in the NE Atlantic (ODP Leg 94) and in the Boso Peninsula (W Pacific). In our material, the FO of *R. asanoi* can be identified at MIS 35 in Core PS2709-1. According to the paleomagnetic record, this FO in Cores PS2709-1 and PS2708-1 is observed at the base of subchron C1r.2r.1r, which correlates with the assigned MIS 35 (Figs. 4–7; Table 4; Appendix Tables A3 and A5). Unfortunately, the low resolution of the stable isotope record precludes calibration in cores PS2487-6 and PS2076-1.

5.8. Last occurrence of large *Gephyrocapsa*

The LO of the large *Gephyrocapsa* morphotype (large *Gephyrocapsa* sp. B — Matsuoka and Okada, 1990; LG, Raffi et al., 1993) is a globally synchronous event that has been recorded in MIS 37 (Raffi et al., 1993; Wei, 1993). In our high latitude sections, it is

well identified in Core PS2709-1 at the same inferred isotope stage. Regarding the paleomagnetic record, this LO occurs in the uppermost portion of subchron C1r.2r.2r in cores PS2709-1 and PS2708-1 (Figs. 4–7; Table 4; Appendix Tables A3 and A5), in agreement with the isotopic calibration. These data confirm the global synchrony of this event.

5.9. First occurrence of large *Gephyrocapsa*

The FO of large *Gephyrocapsa* is a diachronous event. Raffi et al. (1993) placed this event between MIS 46 and 49 and Wei (1993) observed the same event from MIS 47 to 51. In our cores, this event is not well calibrated due to the absence of age-control points (Figs. 2–7; Appendix Tables A1–A5). However, as observed in Figs. 4 and 5 (Appendix Table A3 and A5), this event is situated between the normal geomagnetic subchrons C1r.2r.1n and C2n (between 1.757 and 1.212 Myr — after Cande and Kent, 1992).

Other events used in low- and mid-latitude Pleistocene stratigraphy, such as the LO of *Helicosphaera sellii* (Raffi et al., 1993; Wei, 1993), are difficult to identify in high latitudes because this taxon only occurs sporadically.

6. Conclusions

Ten Pleistocene calcareous nannofossil events calibrated with oxygen isotope and paleomagnetic stratigraphies and correlated with low and middle latitude stratigraphies are discussed.

The events identified are based on some species of Noelaerhabdaceae (*Reticulofenestrids*), which are cosmopolitan and facilitate correlations between high, middle, and low latitudes.

“Standard” events such as the FO of *Emiliana huxleyi* and the LO of *Pseudoemiliana lacunosa*, calibrated by Thierstein et al. (1977) at MIS 8 and 12, respectively, are recorded at the same levels in our cores, demonstrating they are globally synchronous events.

Other events observed in different latitudes and oceans identified and calibrated here include:

- (a) A reversal in the abundance of *Gephyrocapsa muelleriae/E. huxleyi* at the MIS 4/5 boundary. This

event is diachronous in comparison with the existing low-latitude and North Atlantic data.

(b) The FCO of *G. muelleriae* is identified at MIS 6, showing a good synchronism according to the references for other oceanic areas.

(c) The LCO of *Gephyrocapsa caribbeanica*, another globally synchronous event, is also observed in our material at MIS 7.

(d) The FCO of *G. caribbeanica*, although not well documented, in our cores occurs from the MIS 13/14 boundary to MIS 13, showing a slight diachronism.

(e) We corroborate the global synchronism of The LO of *Reticulofenestra asanoi* observed at MIS 22.

(f) The re-entry of medium *Gephyrocapsa* (= *G. parallela*) occurs in the area studied at MIS 25, but is clearly diachronous with existing calibrations for other oceanic areas.

(g) The FO of *R. asanoi* observed at MIS 35 is another diachronous event that has been reported to occur at younger ages in low latitudes of the Pacific and Atlantic Oceans.

(h) The LO of large *Gephyrocapsa* is a global synchronous event that has also been identified at MIS 37 in the Southern Ocean.

Some of the problems arising in establishing an accurate biostratigraphic framework for high latitudes hinge on the ecological restriction of some marker species, scarce in high latitudes. Calcium carbonate dissolution is another factor that, “a priori”, may alter the stratigraphic pattern due to the disappearance of specimens or diagnostic features for identification. Additionally, calcareous nannofossil dilution in an organic siliceous matrix and reworking may also be an important factor in the identification of nannofossil events, especially as regards quantitative and/or semi-quantitative data (e.g. Gard and Crux, 1991; Roth, 1994).

Acknowledgements

The authors wish to express their thanks to Dr Alexandra Negri and Dr Kazuhiro Sugiyama for their valuable review and suggestions. N.S.D. Skinner is acknowledged for revising the English version of

the MS. Isotope measurements were accomplished in the AWI isotope laboratory under the helpful guidance of Dr A. Mackensen. Research grants CICYT ANT97-1909-E, CLI-1002-CO2-02 and the Spanish–German Integrated Actions supported this study.

Appendix A. Taxonomic appendix

Calcareous Nannofossils

- Calcidiscus leptoporus* (Murray and Blackman, 1898) Loeblich and Tappan, 1978
Emiliania huxleyi (Lohmann, 1902) Hay and Mohler in Hay et al., 1967
Gephyrocapsa aperta Kamptner, 1963
Gephyrocapsa caribbeanica Boudreaux and Hay, 1967
Gephyrocapsa ericsonii McIntyre and Bé, 1967
Gephyrocapsa muelleriae Bréhéret, 1978
Gephyrocapsa oceanica Kamptner, 1943
Gephyrocapsa omega Bukry, 1973
Gephyrocapsa parallela (Hay and Beaudry, 1973)
Helicosphaera sellii (Bukry and Bramlette, 1969)
Pseudoemiliania lacunosa (Kamptner, 1963) Gartner, 1969
Reticulofenestra asanoi Sato and Takayama, 1992

Planktonic Foraminifera

- Neogloboquadrina pachyderma* (Ehrenberg, 1861)

Tables A1–A5.

Abundance of marker species and morphotypes used in the studied cores. Total abundance of the calcareous nannofossil assemblage for each sample, observed at a magnification of 1250×, was estimated as follows: A = >50 nannoliths per field of view, C = 1 – 50 nannoliths per field of view. Samples with less than one specimen per field of view are not included in the tables. The ranking of preservation was established as: G = good, M = moderate, and P = poor. The relative abundances of taxa or morphotypes were estimated as follows: V = very abundant (>50%); A = abundant (>20 <50%); C = common (>10 <20%); F = few (>1 <10%); R = rare (<1%).

Table A1
Core PS2487-6

Depth (cm)	Abundance	Preservation	<i>Emiliana luxleyi</i>	Small <i>Gephyrocapsa</i>	<i>Gephyrocapsa muellerae</i>	<i>Gephyrocapsa oceanica</i>	<i>Gephyrocapsa caribbeanica</i>	<i>Pseudoemiliana lacunosa</i>	Medium <i>Gephyrocapsa</i>	<i>Reticulofenestra asanoi</i>	Large <i>Gephyrocapsa</i>
3	A	G	A	C	F	F					
10	A	G	A	C	F	C					
20	A	G	V	F	F	F					
25	A	G	A	A	F	C					
35	A	G	A	C	C	F					
45	A	G	A	C	C	C					
55	A	G	A	C	A	F					
65	A	G	C	C	C	C					
75	A	G	A	A	A	C					
80	A	G	C	C	C	C					
90	A	G	A	A	A	C	R				
100	A	G	C	C	F	C					
110	A	G	A	A	C	C	R				
120	A	G	C	C	F	A	R				
130	A	G	C	C	A	A					
140	A	G	C	A	A	C	R				
150	A	G	C	A	C	C	R				
160	A	G	C	A	F	A	R				
170	A	G	F	A	F	A	R				
180	A	G	F	A	F	A	R				
190	A	G	C	V	F	C	F				
200	A	G	R	A	F	C	C				
210	A	G	R	A	C	F	A				
220	A	G		V	F	R	A				
230	A	G		V	C	R	A				
240	A	G		A	C	R	V				
250	A	G		A	F	R	V				
260	A	G		A	F		V				
270	A	G		A	F	R	V				
280	A	G		A	F	R	V				
300	A	G		A	F	R	V				
310	A	G		A	F	R	V				
320	A	G		A	F	R	V				
330	A	G		A	F	R	V				
340	A	G		V	F	R	A				
370	A	G		V	F	R	V				
380	A	G		A	F	R	V				
390	A	G		A	F		V				
400	A	G		A	F		V				R
410	A	G		A	F	R	V				R
420	A	G		V		F	V				R
430	A	G		V	R	R	V				R
440	A	G		V		R	C		R		
450	A	G		A	R	R	V				R
460	A	G		A	R	R	A				F

Table A1 (continued)

Depth (cm)	Abundance	Preservation	<i>Emiliana huxleyi</i>	Small <i>Gephyrocapsa</i>	<i>Gephyrocapsa muelleriae</i>	<i>Gephyrocapsa oceanica</i>	<i>Gephyrocapsa caribbeana</i>	<i>Pseudoemiliana lacunosa</i>	Medium <i>Gephyrocapsa</i>	<i>Reticulofenestra asanoi</i>	Large <i>Gephyrocapsa</i>
465	A	G		V	R	F	A	F			
470	A	G		V	R	F	R	C	R		
495	A	G		A		F	R	A	F		
505	A	G		A	R	F	R	A		F	
515	A	G		A		F	F	A	F		
525	A	G		V	R	C		C	R	R	
535	A	G		V		F		F	F	R	
545	A	G		V	R			F	F	F	
555	A	G		V		F		C	F		
565	A	G		V	F		R	C	F	C	
575	A	G		V	F	F	R	C	R		
585	A	G		V	R		F	R	F		
595	A	G		V		R	R	R	R		
605	A	G		V	R			R	R	R	
615	A	G		V		R	R	R			
625	A	G		V	R			R	R	R	
635	A	G		V		R	R	R	R		
645	A	G		V		R		R	R	F	
655	A	G		V	R	R	R	F	R	R	
665	A	G		V	R	R	R	F	F	F	
675	A	G		V		R	R	A		R	
685	A	G		A	R			C		A	
695	A	G		V	F	R	R	A	R	F	
705	A	G		A				C	F	C	
715	A	G		C	F			C	C	A	
725	A	G		C	F			C	F	A	
735	A	G		V	F	R	R	C	C	C	
745	A	G		V	F			C	R	C	
755	A	G		V	R	F		C	R	C	
765	A	G		V	F			C	R	F	
775	A	G		V	R	R		F		F	
785	A	G		V	R	R	R	C	R	F	
795	A	G		V				A		C	
805	A	G		V				F	R	C	
815	A	G		V				C		F	
835	A	G		A				C		A	
855	A	G		V				F		R	
865	A	G		V				A		F	
875	A	G		C				A		F	
895	A	G		V				A		R	
905	A	G		V				C		F	
915	A	G		V				A			
935	A	G		A				A			R
955	A	G		V				A			F
974	A	G		V		R		A			F
995	A	G		V		R		C			F

Table A1 (continued)

Depth (cm)	Abundance	Preservation	<i>Emiliana huxleyi</i>	Small <i>Gephyrocapsa</i>	<i>Gephyrocapsa muelleriae</i>	<i>Gephyrocapsa oceanica</i>	<i>Gephyrocapsa caribbeanica</i>	<i>Pseudoemiliana lacunosa</i>	Medium <i>Gephyrocapsa</i>	<i>Reticulofenestra asanoi</i>	Large <i>Gephyrocapsa</i>
1015	A	G		V		R		A			F
1035	A	G		V		R		F			F
1055	A	G		A		F	F	A			A
1073	A	G		A		F	C	C			A
1095	A	G		A		F	A	A			
1115	A	G		A		R	C	A			
1135	A	G		F				A			
1155	A	G		R				A			
1175	A	G						C			
1195	A	G						A			
1215	A	G						A			
1235	A	G						A			
1255	A	G						A			

Table A2
Core PS2076-1

Depth (cm)	Abundance	Preservation	<i>Gephyrocapsa huxleyi</i>	Small <i>Gephyrocapsa</i>	<i>Gephyrocapsa muelleriae</i>	<i>Gephyrocapsa oceanica</i>	<i>Gephyrocapsa caribbeanica</i>	<i>Pseudoemiliana lacunosa</i>	Medium <i>Gephyrocapsa</i>	<i>Reticulofenestra asanoi</i>	Large <i>Gephyrocapsa</i>
0	A	G	A	F	F	C					
7	A	G	A	F	F	F					
17	A	G	V	F	F	F					
27	A	G	A	F	F	F					
37	A	G	A	F	C	F					
46	A	G	A	F	A	F					
57	A	G	C	F	V	C					
67	A	G	C	F	A	F					
77	A	G	V	F	F	F					
87	A	G	A	F	A	R					
97	A	G	A	F	C	F					
107	A	G	C	C	C	C					
127	A	G	C	F	C	C					
137	A	G	F	A	F	C					R
147	A	G	R	C		A					R
157	A	G	R	V		C					
167	A	G	R	V							C
177	A	G	F	C		R					F
187	A	G	F	A		C					C
197	A	G		A		C					A

Table A2 (continued)

Depth (cm)	Abundance	Preservation	<i>Gephyrocapsa huxleyi</i>	Small <i>Gephyrocapsa</i>	<i>Gephyrocapsa muelleriae</i>	<i>Gephyrocapsa oceanica</i>	<i>Gephyrocapsa caribbeanica</i>	<i>Pseudoemiliana lacunosa</i>	Medium <i>Gephyrocapsa</i>	<i>Reticulofenestra asanoi</i>	Large <i>Gephyrocapsa</i>
207	A	G		C		F	A				
217	A	G		C		F	A				
227	A	G		C			A				
257	A	G		A			A				
297	A	G		A			V				
307	A	G		C		F	A	R			
327	A	G		A			A	C	R		
337	A	G		A		F	A	F			
347	A	G		C			A	C			
357	A	G		C			C	C			
367	A	G		A		F	F	R	C		
377	A	G		A				R	C		
387	A	G		A		F		C			
487	A	G		A				F	C		
547	A	G		V		F		C	C		
577	A	G		A				F	C		
587	A	G		A				C	F	F	
599	A	G		A				C	C	C	
637	A	G		A				C	F	C	
647	A	G		V				A	C	C	
657	A	G		A				A		C	
667	A	G		A				A		C	
677	A	G		A				C		A	
717	A	G		V				C		V	
737	A	G		A				C		C	
747	A	G		V				A		C	
757	A	G		A				C		F	
767	A	G		A				V		?	
777	A	G		C				A			R
789	A	G		C				A	R		F
797	A	G		A				C	F		C
807	A	G		A				C	F		C
817	A	G		A				C	C		C
827	A	G		A				C	C		C
857	A	G		C				C	C		A
888	A	G		C				C	V		F
897	A	G		F				C	C		
907	A	G		C				C	A		R
917	A	G		C				C	C		
927	A	G		C				C	C		
937	A	G		C				A	F		
947	A	G		C				C	F		
957	A	G		F				F			
977	A	G		F				C			
987	A	G		F				C			

Table A3
Core PS2709-1

Depth (cm)	Abundance	Preservation	<i>Emiliana huxleyi</i>	Small <i>Gephyrocapsa</i>	<i>Gephyrocapsa muelleriae</i>	<i>Gephyrocapsa oceanica</i>	<i>Gephyrocapsa caribbeanica</i>	<i>Pseudoemiliana lacunosa</i>	Medium <i>Gephyrocapsa</i>	<i>Reticulofenestra asanoi</i>	Large <i>Gephyrocapsa</i>
20	A	G	A	F	R						
50	A	G	A	C	C						
100	A	G	V	F	C						
120	A	G	A	F	A						
130	A	G		A	C						
140	A	G	R	C	C	F					
145	A	G	R	C		R	C				
150	C	M	R	F			F				
155	A	G		C			A				
160	A	G		C			C				
169	A	G		C			C				
180	A	G		V			A				
250	A	G		A			V				
300	A	G		C		C	V				
350	A	G		A			V				
370	A	G		A			A				
380	A	G		A			A				
390	A	G		A			A	R	C		
395	A	G		C			A	F	R		
400	A	G		C			A	F	F		
410	A	G		A			C	F	C		
420	A	G		C			C	C	C		
422	F	M		C			R			R	
430	A	G		C			F				
450	A	M		A		R	F		A		
500	F	M		R			F	R	R		R
550	A	G		V			F	R	R		R
600	A	G		F			C	R			R
650	A	G		V			F				
700	C	M		C			F			R	
710	A	G		V			F	R			
720	A	G		A			F	R		R	
725	A	G		V			C				
730	A	G		V			F	R		F	
740	A	G		V			F			F	
750	F	M		F			F	R		R	
755	F	M					R			R	
760	F	M		R			F	R		R	
770	A	G		A			F	F		F	
780	A	M		F			F			F	
820	C	M		F			R			F	
850	C	M		F			F			F	
860	C	M		R			R			R	
870	C	M		C			F			R	
890	C	M		R			R			R	
920	C	M		F			R			F	
930	A	G		V			F			C	
950	A	G		V			F			F	
960	A	G		V			R			R	
965	A	G		V			C			F	

Table A3 (continued)

Depth (cm)	Abundance	Preservation	<i>Emiliana huxleyi</i>	Small <i>Gephyrocapsa</i>	<i>Gephyrocapsa muelleræ</i>	<i>Gephyrocapsa oceanica</i>	<i>Gephyrocapsa caribbeana</i>	<i>Pseudoemiliana lacunosa</i>	Medium <i>Gephyrocapsa</i>	<i>Reticulofenestra asanoi</i>	Large <i>Gephyrocapsa</i>
970	C	M		R				F		C	
1000	C	M		R				C		F	
1040	F	M						A		R	
1050	C	M		R				C		F	
1060	F	M						C		R	R
1065	C	M						C			R
1070	C	M						C		R	
1080	C	M						F			
1090	F	M						F	?		R
1095	F	M						F	R		C
1100	F	M		R				F	R		F
1105	F	M						F			
1110	F	M						A	F		C
1115	F	M						C	C		C
1120	F	M						F	F		C
1130	C	M		R				F	F		C
1140	C	M						F	F		C
1200	C	M		R				F	R		C
1230	C	M		R				F	F		F
1250	A	G		A				F	A		A
1260	A	G		F				R	F		C
1270	C	G						C	C		F
1275	A	G						C	A		F
1280	C	M		R				R	F		
1290	C	M		A				R	F		
1300	C	M		F				F	F		
1310	C	M		F				F	F		
1315	C	M		F				R	F		
1320	F	M		F				F			
1340	F	M		F				F			
1400	C	M						F			
1500	C	M						F			
1540	C	M		F				F			
1550	C	M						R			
1560	C	M						R			
1570	C	M						F			
1600	C	M						F			
1620	C	M						F			
1640	C	M						F			
1650	C	M						F			
1660	C	M						F			
1668	C	M						F			

Table A4
Core PS2703-1

Depth (cm)	Abundance	Preservation	<i>Emiliana huxleyi</i>	Small <i>Gephyrocapsa</i>	<i>Gephyrocapsa muelleriae</i>	<i>Gephyrocapsa oceanica</i>	<i>Gephyrocapsa caribbeanica</i>	<i>Pseudoemiliana lacunosa</i>	Medium <i>Gephyrocapsa</i>	<i>Reticulofenestra asanoi</i>	Large <i>Gephyrocapsa</i>
58	A	G	V	F	F						
68	A	G	V		R	R					
78	A	G	V	F	C	R					
88	A	G	A		A						
98	A	G	F		V						
108	A	G	C	F	R						
128	A	G	F	C	C	F					
138	A	G	F	A			C				
148	A	G			F		C				
188	A	G		A			A				
246	A	G		A			C				
348	A	G		A			A	R			
408	A	G		F			A				
428	A	G		F			F				
438	A	G		F			F	F			
448	A	G		F			R				
458	A	G		F		R		F			
468	C	G		F			F	F			
488	A	G		R				R			
528	A	G		R				R			
578	A	G		C				F			
638	A	G		F				F			
778	A	G		V				F			
788	A	G		C		R		F		R	
798	A	G		F				F			
808	A	G		A		C		F		R	
818	A	G		F				F			
828	A	G						C		F	
838	A	G		F				F	R	F	
888	A	G		C				F	R	F	
898	A	G		F					R	F	
908	A	G		F				F	R		
918	A	G						F	R		
928	A	G		F						R	
963	A	G		C				F		F	
993	A	G		F				F		R	
1053	A	G		V				F		F	
1063	A	G		V				F		F	
1073	A	G		F				F		R	
1083	A	G		C				F		R	
1093	A	G		F				F		R	
1103	A	G						F		R	
1113	A	G						C		R	
1123	A	G						C		R	

Table A4 (continued)

Depth (cm)	Abundance	Preservation	<i>Emiliana huxleyi</i>	Small <i>Gephyrocapsa</i>	<i>Gephyrocapsa muelleriae</i>	<i>Gephyrocapsa oceanica</i>	<i>Gephyrocapsa caribbeana</i>	<i>Pseudoemiliana lacunosa</i>	Medium <i>Gephyrocapsa</i>	<i>Reticulofenestra asanoi</i>	Large <i>Gephyrocapsa</i>
1173	A	G						C			
1233	A	G						F			
1240	A	G						F			F
1250	A	G						F	F		C
1300	A	G						C	F		C
1310	A	G						F	F		F
1320	A	G						F	C		F
1330	A	G						F	C		C
1340	A	G		R				F	C		C
1410	A	G		R				F	C		C
1480	A	G		R					F		F
1490	A	G		F					F		F
1500	A	G									F
1510	A	G							F		F
1520	A	G							F		
1530	A	G						F	F		
1590	A	G		F				F	F		
1600	A	G		R				F			
1610	A	G		R				F	R		
1620	A	G						F	F		
1630	A	G						F	F		
1640	A	G						F	R		
1650	A	G		R				C			
1660	A	G		F				F	R		
1670	A	G						F			
1680	A	G						F			
1690	A	G		F				F			
1700	A	G		F				F			
1730	A	G		R				F			

References

- Bathmann, U., Schulz-Baldes, M., Fahbach, E., Smetacek, V., Hubberten, H.-W., 1992. Die Expedition ANTARKTIS IX/1-4 des Forschungsschiffes Polarstern 1990/91. Ver. Polarforsch., vol. 100, p. 403.
- Bolli, H.M., Ryan, W.B.F., et al., 1978. Init. Repts. Deep Sea Drilling Project, 40.
- Bollmann, J., 1977. Morphology and biogeography of the genus *Gephyrocapsa* coccoliths, in Holocene sediments. Mar. Micropaleontol. 29, 319–350.
- Bollmann, J., Baumann, K.H., Thierstein, H.R., 1998. Global dominance of *Gephyrocapsa* coccoliths in the late Pleistocene: selective dissolution, evolution, or global environmental change? Paleogeography 13, 517–529.
- Br  h  ret, J.G., 1978. Formes nouvelles quaternaires et actuelles de la famille Gephyrocapsaceae (Coccolithophoridae). C.R. Acad. Sci. Paris, Ser. D 287, 447–449.
- Bukry, D., 1973. Coccolith stratigraphy — eastern equatorial Pacific, Leg 16, Deep Sea Drilling Project. Init. Repts. Deep Sea Drilling Project 16, 653–712.
- Cande, S.C., Kent, D.V., 1992. A new geomagnetic polarity time scale for the Late Cretaceous and Cenozoic. J. Geophys. Res. 97, 13917–13951.
- Crux, J.A., 1991. Calcareous nannofossils recovered by Leg 114 in the Subantarctic South Atlantic Ocean. Proc. Ocean Drilling Program, Sci. Results 114, 155–177.
- Flores, J.A., Gersonde, R., Sierro, F.J., 1999. Pleistocene fluctuations in the Agulhas Current Retroflexion based on the calcareous plankton record. Mar. Micropaleontol. 37, 1–22.
- Gard, G., 1989. Quaternary calcareous nannofossil biostratigraphy: the eastern Arctic Ocean record. In: Herman, Y. (Ed.), The Arctic Seas. Climatology, Oceanography, Geology and Biology. Van Nostrand Reinhold, New York, pp. 445–459.
- Gard, G., Crux, J., 1991. Preliminary results from Hole 704A: Arctic–Antarctic correlation through nannofossil biochronology. Proc. Ocean Drilling Program, Sci. Results 114, 193–200.
- Gartner, S., 1977. Calcareous nannofossil biostratigraphy and revised zonation of the Pleistocene. Mar. Micropaleontol. 2, 1–25.
- Gersonde, R., et al. 1995. The Expedition ANTARKTIS-XI/2 of RV *Polarstern*, in 1993/94, Berichte zur Polarforschung, vol. 163, pp. 1–133.
- Gersonde, R., Kyte, F.T., Bleil, U., Diekmann, B., Flores, J.A., Gohl, K., Grahl, G., Hagen, R., Kuhn, G., Sierro, F.J., V  lker, D., Abelman, A., Bostwick, J.A., 1997. Geological record and reconstruction of the late Pliocene impact of the Eltanin asteroid in the Southern Ocean. Nature 390, 357–363.
- Giraudeau, J., Pujos, A., 1990. Fontion de transfer bes  e sur les nannofossiles calcaires du Pleistoc  ne des Caribes. Oceanol. Acta 13, 453–469.
- Hine, N., Weaver, P.P.E., 1998. Quaternary. In: Bown, P.R. (Ed.), Calcareous nannofossil Biostratigraphy. Chapman and Hall, London, pp. 266–283.
- Hut, G. 1987. Stable isotope reference samples for geochemical and hydrological investigations, report to the Director General, 42pp, International Atomic Energy Agency, Vienna, September 16–18.
- Jordan, R.W., Zhao, M., Eglinton, G., Weaver, P.P.E., 1996. Coccolith and alkenone stratigraphy and paleoceanography at an upwelling site off NW Africa (ODP 658C) during the last 130,000 years. In: Whatley, R., Mognilevsky, A. (Eds.), Microfossils and Oceanic Environments. Aberystwyth-Press, Aberystwyth, pp. 111–130 (University of Wales).
- Kennet, J.P., Barron, J.A., 1992. Introduction. In: Kennet, J.P., Warnke, D.A. (Eds.), The Antarctic Paleoenvironment: A Perspective on Global Change, vol. 56. American Geophysical Union, Washington, DC, pp. 1–6.
- Martini, E., 1971. Standard Tertiary and Quaternary calcareous nannoplankton zonation. In: Farinacci, A. (Ed.), Proceedings of the Second Olanktonic Conference Roma (1970), vol. 2. Edizioni Technoscienza, Rome, pp. 739–785.
- Matsuoka, H., Okada, H., 1990. Time-progressive morphometrical changes of the genus *Gephyrocapsa* in the Quaternary sequence of the tropical Indian Ocean Site 709. Proc. Ocean Drill. Program, Sci. Results 115, 255–270.
- Niebler, S., 1995. Rekonstruktionen von Pal  o-Umweltparametern anhand von stabilen Isotopen und Faunen-Vergesellschaftungen planktischer Foraminiferen im S  datlantik. Berichte zur Polarforschung 167, 1–198.
- Novaczky, N.R., Baumann, M., 1992. Combined high-resolution magnetostratigraphy and nannofossil biostratigraphy for late Quaternary Arctic Ocean sediments. Deep-Sea. Res. 39, 567–601.
- Okada, H., Bukry, D., 1980. Supplementary modification and introduction of code numbers to the low-latitude coccolith biostratigraphic zonation (Bukry, 1973; 1975). Mar. Micropaleontol. 5, 321–325.
- Pujos-Lamy, A., 1977. *Emiliania* et *Gephyrocapsa* (Nannoplankton calcaire): Biometrie et interet biostratigraphique dans le Pleistocene superieur marin des A  ores. Revista Espa  ola de Micropaleontolog  a 9, 69–84.
- Pujos, A., Giraudeau, J., 1993. Repartition des Noelaerhabdaceae (nannofossils calcaires) dans le Quaternaire moyen et superieur des oceans Atlantique et Pacifique. Oceanolog. Acta 16, 349–362.
- Raffi, I., Flores, J.A., 1995. Pleistocene trough Miocene calcareous nannofossils from eastern equatorial Pacific Ocean (Leg 138). Proc. Ocean Drilling Program, Sci. Results 138, 233–286.
- Raffi, I., Backman, J., Rio, D., Shackleton, N.J., 1993. Plio-Pleistocene nannofossil biostratigraphy and calibration to oxygen isotope stratigraphies from Deep Sea Drilling Project Site 607 and Ocean Drilling Program Site 677. Paleogeography 8, 387–408.
- Roth, P.H., 1994. Distribution of coccoliths in oceanic sediments. In: Winter, A., Siesser, W.G. (Eds.), Coccolithophores. Cambridge University Press, Cambridge, pp. 199–218.
- Santleben, C., 1980. Die Evolution der Coccolithophoriden-Gattung *Gephyrocapsa* nach Befunden im Atlantk. Pal  ont. Z. 54, 91–127.
- Sato, T., Takayama, T., 1992. A stratigraphical significant new species of the calcareous nannofossil *Reticulofenestra asanoi*. In: Ishizaki, K., Saito, T. (Eds.), Centenary of Japanese Micropaleontology, Terra Scientific, Tokyo, pp. 457–460.
- Shipboard Scientific Party, 1999. Legsummary: Southern Ocean

- paleoceanography. In: Gersonde, R., Hodell, D., Blum, P. Proc. Ocean Drilling Program, Inits. Repts., 177: College Station, TX (Ocean Drilling Program), pp. 1–67.
- Takayama, T., Sato, T., 1987. Coccolith biostratigraphy of the North Atlantic Ocean, Deep Sea Drilling Project Leg 94. Init. Repts. DSDP 94, 651–702.
- Tiedemann, R., Sarthein, M., Shackleton, N.J., 1994. Astronomic timescale for the Pliocene Atlantic $\delta^{18}\text{O}$ and dust flux records of Ocean Drilling Program site 659. *Paleoceanography* 9 (4), 619–638.
- Thierstein, H.R., Geitzenauer, K.R., Molino, B., Shackleton, N.J., 1977. Global synchronicity of late Quaternary coccolith datum levels: validation by oxygen isotopes. *Geology* 5, 400–404.
- Weaver, P.P.E., 1983. An integrated stratigraphy of the Upper Quaternary of the King's Trough flank area EN Atlantic. *Oceanol. Acta* 6 (4), 451–456.
- Weaver, P.P.E., Thomson, J., 1993. Calculating erosion by deep-sea turbidity currents during initiation and flow. *Nature* 364, 136–138.
- Wei, W., 1993. Calibration of Upper Pliocene–Lower Pleistocene nannofossil events with oxygen isotope stratigraphy. *Paleoceanography* 8, 85–99.
- Wei, W., Wise, S.W., 1992. Oligocene–Pleistocene calcareous nannofossils from Southern Ocean Sites 747, 748 and 751. *Proc. Ocean Drilling Program Sci. Results* 120, 368–373.
- Wells, P., Okada, H., 1997. Response of nannoplankton to major changes in sea-surface temperature and movements of hydrological fronts over Site DSDP 594 (south Chatham Rise, south-eastern New Zealand), during the last 130 kyr. *Mar. Micropaleontol.* 32, 341–363.
- Wise, S.W., 1983. Mesozoic and Cenozoic calcareous nannofossils recovered by Deep Sea drilling Project Leg 71 in the Falkland Plateau region, southwest Atlantic Ocean. *Inits. Repts. DSDP* 71, 481–550.
- Wise, S.W., Wind, F.H., 1977. Mesozoic and Cenozoic calcareous nannofossils recovered by DSDP Leg 36 drilling on the Falkland Plateau, southwest Atlantic sector of the Southern Ocean. *Init. Repts. DSDP* 36, 269–492.